Nuclear Instruments and Methods in Physics Research A 671 (2012) 144–149

Contents lists available at SciVerse ScienceDirect

Nuclear Instruments and Methods in Physics Research A

journal homepage: www.elsevier.com/locate/nima

Development and characterization of a 3D CdTe:Cl semiconductor detector for medical imaging

Marie-Laure Avenel [a], Daniel Farcage [b], Marie Ruat [a], Loïck Verger [a], Eric Gros d'Aillon [a,*]

[a] CEA, LETI, MINATEC-Campus, 17 rue des Martyrs, F-38054 Grenoble, France
[b] CEA, DEN-DPC, F-91191 Gif Sur Yvette, France

ARTICLE INFO

Article history:
Received 10 May 2011
Received in revised form
26 October 2011
Accepted 21 November 2011
Available online 27 December 2011

Keywords:
3D semiconductor detectors
Medical imaging
CdTe
Laser drilling

ABSTRACT

Conventional semiconductor radiation detectors for medical imaging use either a planar structure or a pixelated structure. These structures exhibit a natural trade-off between the absorption of incident photons and the collection of free charge carriers, resulting in a limited choice of detection materials. Such a trade-off can be avoided using a 3D structure in which electrodes are drilled into the detection volume. A prototype 3D semiconductor detector has been developed, using CdTe:Cl. A laser drilling technique was used to create electrodes in the volume of the material. The electrodes were contacted using electroless Au deposition. The manufacturing process and the first spectrometric results obtained with ^{241}Am and ^{57}Co irradiation are presented below. Synchrotron X-ray irradiation was also performed at the European Synchrotron Radiation Facility (ESRF) at an incident energy of 60 keV. An individual photon-counting ability was exhibited. These results will be used as a proof of concept for investigating 3D detectors in the medical-imaging energy range.

1. Introduction

3D detection geometry was first introduced by Parker et al. in 1997 [1]. Whereas in conventional planar or pixelated detection structures electrodes are deposited onto the surface of the detector, 3D structures are made of a three-dimensional array of cylindrical electrodes placed in the detection volume and generally extend through the whole thickness of the detector. These electrodes are alternately biased as cathodes and anodes, as shown in Fig. 1.

In the 3D geometry, photons are usually absorbed along the thickness of the detector, whereas charge collection occurs in the perpendicular direction, in a plane parallel to the surface of the detector.

Doubled-sided 3D silicon sensors [2,3] have been widely studied for high-energy particle detection. The silicon is processed using Reactive Ion Etching (RIE) [4] and laser drilling [5] of electrodes. 3D silicon structures have also been studied for medical imaging applications in the 10–60 keV energy range [6]. The silicon detection layers are usually a few hundred microns thick. However, thicker detection layers are needed to achieve good absorption above 60 keV. Silicon is thus not suitable for the medical imaging applications targeted here, involving an energy level of up to 140 keV. Therefore, an alternative material, such as semi-insulating GaAs, was considered. However, CdTe:Cl was chosen as a proof of concept for 3D-structure development and as a reference point in terms of achievable performances in comparison to existing CdTe planar/pixelated structures. The detector manufacturing process is described below, from the laser drilling of holes into the CdTe:Cl to the electroless deposition of Au contacts along the surface of the holes, read-out circuit connection and characterization under ^{241}Am, ^{57}Co gamma-ray and synchrotron X-ray irradiation.

2. CdTe:Cl 3D detector manufacturing

The CdTe:Cl was provided by Acrorad. The following transport properties were considered: $\mu_{electrons} = 1000\ cm^2/V/s$, $\mu_{holes} = 50\ cm^2/V/s$, $\tau_{electrons} = \tau_{holes} = 1\ \mu s$ [7], that allow for both electrons and holes collection.

Two samples were made.

Sample 1 aimed at checking the laser drilling technique. It consisted of a 60,000-hole matrix drilled into a 1 mm-thick CdTe detector. A hole diameter of 20 μm at a pitch of 100 μm was achieved, i.e., a 50:1 aspect ratio for the holes.

Sample 2 reduced the constraints on the hole diameter and pitch and was our prototype for radiation detection characterization. Several arrays of 3 × 3 holes were drilled in a 1.6 mm thick-CdTe:Cl detector with a hole diameter of 100 μm at a pitch of 350 μm (chosen after simulation [8]).

2.1. Laser-machining

Semiconductor etching techniques, like dry etching, chemical etching or RIE, are mainly developed for silicon [9]. In this case,

* Corresponding author. Tel.: +33 4 38 78 20 87.
E-mail address: eric.grosdaillon@cea.fr (E.G. d'Aillon).

0168-9002/$ - see front matter © 2011 Elsevier B.V. All rights reserved.
doi:10.1016/j.nima.2011.11.058

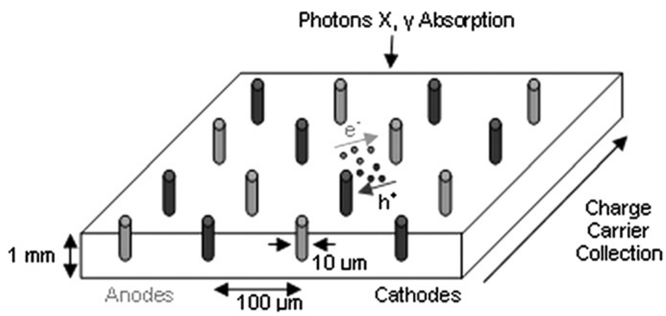

Fig. 1. Diagram of a 3D detector.

holes were laser drilled. Laser-machining is material independent but is a serial process.

The laser drilling was performed at the CEA-Saclay facility. An Nd-YLF pulsed laser was used, exhibiting the following parameters:

- Wavelength=263 nm, enabling a small spot size and small hole diameter.
- Average power=1.95 W.
- Rate=3 kHz.
- Pulse width=41 ns.

The holes, through the whole material thickness, were made by laser beam percussion. During this process, the laser drilling creates a plasma, which contains material particles; these particles can be deposited onto the material surface, near the drilled holes. One hole is drilled in 500 ms.

Sample 1 was observed using an optical microscope and Scanning Electron Microscope (SEM) imaging after Au contacts had been deposited onto the surface of the holes. The sample was cleaved so that the shape of the holes could be studied. Images of sample 1 are presented in Fig. 2.

Fig. 2a shows a detailed view of the top surface of the holes of the sample 1 obtained using an SEM. The sample was polished after Au deposition and exhibits no extra fragment material on the surface. Fig. 2b shows an optical micrograph of the thickness of the detector with contacted holes well-defined over the whole thickness of the detector. Mechanical stress lines caused by the cleavage of the sample can be observed in between the holes. The general shape of the holes is slightly conical, a feature arising from the laser drilling technique. It can also be observed that the Au was properly deposited over the whole surface and the length of the holes. Then, sample 1 was polished along the thickness of the detector and characterized by Scanning Electron Microscopy (Fig. 2c). We can see slightly tapered holes with a hole entrance diameter bigger than the hole exit diameter. A high repeatability of the laser drilling process can also be inferred.

Sample 2 was also observed under optical microscopy. The holes were of an enhanced conical shape (not shown) with an entrance diameter of approximately 100 μm and an exit diameter ranging from 35 to 45 μm. The holes were more tapered due to the larger entrance diameter chosen. The chosen hole diameter and pitch for sample 2 facilitated connection to the read-out electronics, enabling this sample to be used for initial characterization under irradiation.

2.2. Electrode deposition and connection to read-out electronics

Prior to Au deposition, a chemical etch with Br in methanol was performed to remove the material fragments created during the laser drilling process. Au contacts were then deposited on the surface of the holes by electroless deposition from a solution of $AuCl_3$. Finally, the

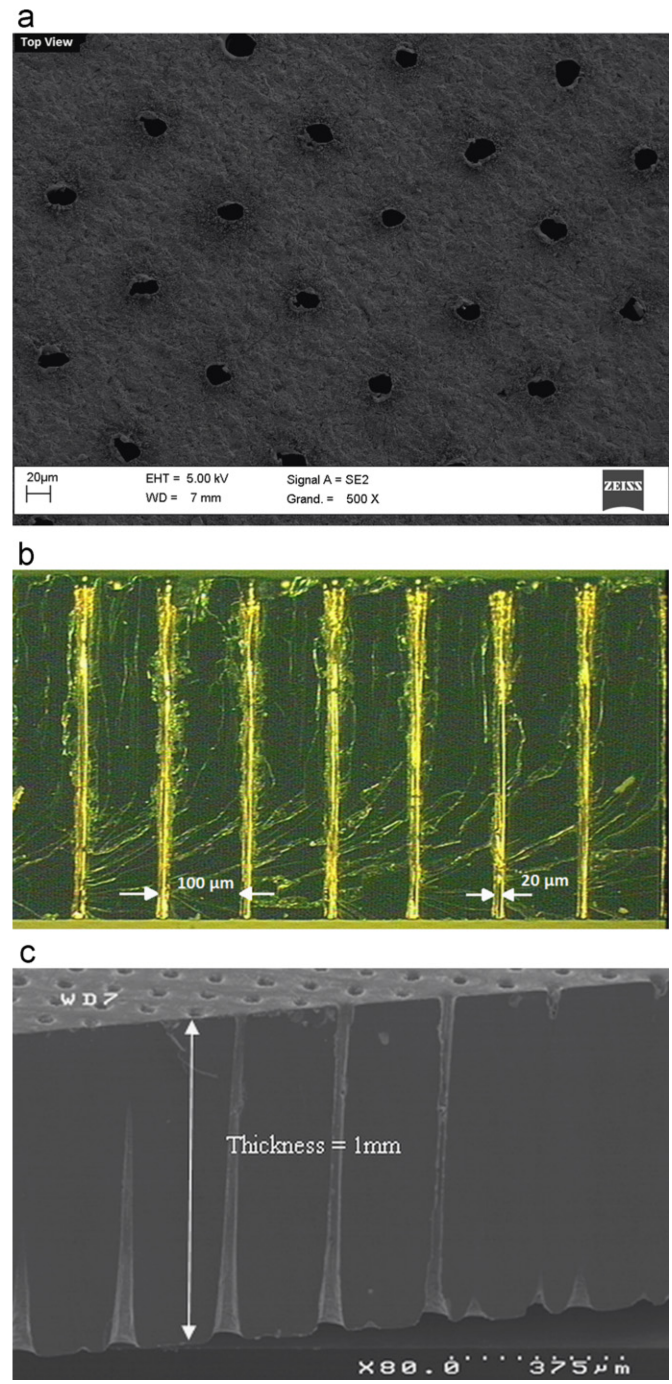

Fig. 2. Sample 1 SEM and optical micrographs of (a) the top surface and (b, c) the thickness of the detector.

top and bottom surfaces of the sample were polished mechanically to remove the Au deposited on these surfaces.

Sample 2 was connected to the read-out electronics using gold wires with diameters of 25 μm, inserted manually into the holes. A suitable electrical contact with acceptable resistivity was expected.

The polarity applied to the wires can be chosen to create different "pixel" arrangements. Fig. 3 shows the two biasing configurations used in this work. From now on, these will be referred to as "diamond-shaped biasing" and "square-shaped biasing". The diamond-shaped biasing arises from connecting the electrodes alternately as cathodes and anodes. In the square-shaped biasing